

Exchange-bias reversal in magnetically compensated ErFeO₃ single crystalI. Fita,^{1,*} A. Wisniewski,¹ R. Puzniak,¹ V. Markovich,² and G. Gorodetsky²¹*Institute of Physics, Polish Academy of Sciences, Aleja Lotnikow 32/46, PL-02-668 Warsaw, Poland*²*Department of Physics, Ben-Gurion University of the Negev, P.O. Box 653, 84105 Beer-Sheva, Israel*

(Received 21 March 2016; revised manuscript received 9 May 2016; published 27 May 2016)

An exchange-bias (EB) effect observed in single crystal ErFeO₃ compensated ferrimagnet, exhibiting the EB field H_{EB} increasing and diverging upon approaching compensation temperature $T_{comp} = 45$ K, and changing sign with crossing T_{comp} , is reported. The EB sign may be changed to the opposite one by varying the field-cooling protocol, depending on whether T_{comp} is crossed with decreasing or increasing temperature. Namely, a different EB sign with the same $|H_{EB}|$ and coercive field H_C values is obtained approaching a given T with increasing and decreasing temperature and the $H_{EB}(T)$ dependence completed in one way is a mirror image of that completed in another way.

DOI: [10.1103/PhysRevB.93.184432](https://doi.org/10.1103/PhysRevB.93.184432)

ErFeO₃ is a representative of the rare-earth orthoferrites that have received renewed attention in recent years because of their attractive properties, promising for applications such as ultrafast spin switching, spin reorientation transition, and multiferroicity [1–4]. Upon cooling, ErFeO₃ shows a sequence of magnetic transitions in the same orthorhombic *Pbnm* perovskite structure. Below the Néel temperature $T_N \approx 636$ K, the Fe³⁺ spins demonstrate the *G*-type antiferromagnetic (AFM) order with slight spin canting, caused by the Dzyaloshinskii-Moriya interaction, resulting in a weak ferromagnetic (FM) moment along the *c* axis. Upon further cooling, the Fe³⁺ spins spontaneously reorient via two subsequent second-order phase transitions starting at 97 K and ending at 88 K, resulting in a reorientation of the FM moment from the *c* axis towards the *a* axis [2,3]. At lower temperature, ErFeO₃ exhibits a magnetic compensation which results from the strong AFM coupling between the Er³⁺ (9.6 μ_B) and Fe³⁺ (5.9 μ_B) magnetic moments. Due to this coupling, the Er³⁺ spins, despite being in a paramagnetic state, develop an alternative canted AFM order with a FM moment opposite to that of the Fe³⁺ spins. The induced Er-sublattice magnetic moment increases with lowering temperature and compensates the moment of Fe³⁺ spins at the compensation temperature $T_{comp} = 45$ K, zeroing the net magnetization [3,4]. Finally, the long-range AFM order of Er³⁺ spins develops below 4.3 K [5]. A recent detailed neutron powder diffraction study [6] well confirms the above spin configurations and magnetic transitions in ErFeO₃, and describes the refined magnetic moments for the Fe³⁺ and Er³⁺ sites, corresponding to the two distinct magnetic sublattices, over the whole temperature range.

Compensated ferrimagnets (fMs) with magnetic moment reversal and negative magnetization have recently attracted further attention because of the occurrence of the exchange-bias (EB) effect [7–12]. Particularly exciting are the giant tunable EB in Heusler alloys [13,14] and recently found extremely high EB up to 4 T in DyCo₄ films [15]. The EB is at present a key instrument for practical applications in magnetic memory and spintronics. Classic EB [16] is associated with interfacial exchange interaction between strongly anisotropic AFM and soft FM phases, leading to a shift in magnetization

hysteresis loop in the direction of the bias field [17]. However, the origin of the EB effect found in a variety of fMs [7–12] near T_{comp} seems to be very different from that of the traditional EB requiring the FM/AFM interface. It is expected that the strong unidirectional anisotropy, originating from the intrinsic exchange coupling within the unit cell, should refer to atomic EB [7,15]. It has been pointed out in Ref. [7] that the unidirectional anisotropy inversely proportional to the net FM moment occurs at the T_{comp} of the fM comprising two antiferromagnetically coupled sublattices. The most interesting finding is that the EB of the compensated fMs reverses its sign across the T_{comp} ; moreover, it may be tuned by applied magnetic field and temperature [11,12]. This striking feature is useful for applications and may help to improve the understanding of the microscopic origin of EB anisotropy. In this paper, we show that the EB sign in a ErFeO₃ fM may be changed to the opposite one by varying the field-cooling protocol; moreover, the negative EB is compatible with the equilibrium spin configuration and the positive one with the metastable state. This novel feature provides deeper insight into the nature of EB in compensated fMs.

Magnetization measurements were performed on ErFeO₃ single crystal with the size of 4.3 \times 3.3 \times 1.6 mm³ in the temperature range 10–250 K and in magnetic fields up to 10 kOe, using a PAR (Model 4500) vibrating sample magnetometer. Figure 1(a) presents the temperature dependence of magnetization of ErFeO₃ measured at 100 Oe along the *a* and *c* axes for zero-field-cooling (ZFC), field-cooling (FC), and field-cooling-warming (FCW) modes. One can recognize two successive magnetic phase transitions. The spin reorientation of the magnetically ordered Fe³⁺ ions proceeds via a continuous rotation of the easy axis [18]. This rotation begins at $T_1 = 86$ K with the weak ferromagnetic moment along the orthorhombic *a* axis and ends at $T_2 = 97$ K with the moment along the *c* axis. An additional phase transition is linked to the FM moment reversal along the *a* axis at crossing the $T_{comp} = 45$ K. The first-order nature of the last one is evidenced by clear hysteresis in FC and FCW magnetization, representing metastable states with magnetic moments opposed to the applied field (negative magnetization) that appear when crossing T_{comp} in both cooling and warming regimes [see inset to Fig. 1(a)]. Noteworthy, very similar metastable spin configurations around the first-order

*Corresponding author: ifita@ifpan.edu.pl

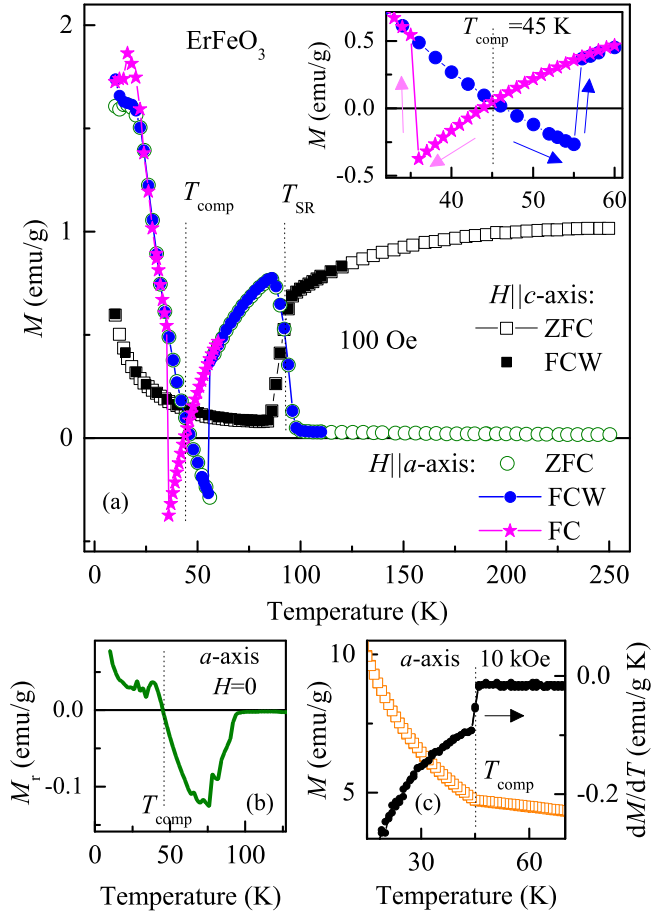


FIG. 1. (a) Temperature dependence of magnetization of ErFeO_3 single crystal measured at 100 Oe along both the a and c axes for zero-field-cooling (ZFC), field-cooling (FC), and field-cooling-warming (FCW) modes. The inset shows the “butterfly” behavior (hallmark of the first-order transition) around the compensation point T_{comp} in an extended scale. (b) Remanent magnetization M_r recorded at $H = 0$ after FC in 10 kOe. (c) Jump in slope dM/dT at T_{comp} for FC magnetization at 10 kOe.

transition temperature T_{comp} have been proved by the x-ray magnetic circular dichroism spectra for the isostructural fM SmMnO_3 [19]. The net magnetic moment along the a axis, dominated by Fe^{3+} spins above T_{comp} and by Er^{3+} spins below T_{comp} , is fully compensated at T_{comp} , indicated by zero low-field magnetization and remanent magnetization M_r [see Fig. 1(b)]. Note that M_r reverses sign at T_{comp} , as expected. In contrast, the high-field (10 kOe) magnetization, involving a large contribution from the AFM coupled spins, shows a distinct discontinuity in the slope dM/dT at T_{comp} , and it demonstrates also the Curie-Weiss-like increase in the field-induced paramagnetic moment of Er sublattice below T_{comp} [see Fig. 1(c)].

Figure 2 shows the angular dependence of the magnetization $M(\theta)$ taken for several temperatures between 40 and 100 K, measured along the direction of applied magnetic field $H = 100$ Oe rotated in the ac plane. It appears that at temperatures close to T_{comp} , i.e., at $T = 40$ and 50 K, the FM moment keeps its initial direction along the easy axis even for a magnetic field with opposite alignment, resulting

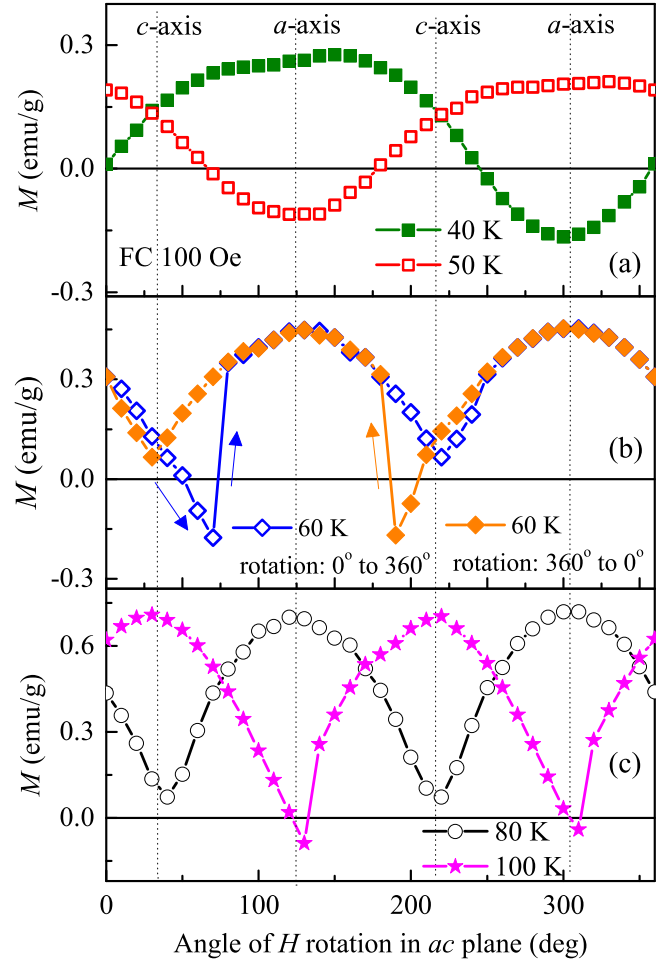


FIG. 2. Angular dependence of the magnetization of ErFeO_3 measured for several temperatures along the applied magnetic field $H = 100$ Oe in the ac plane.

in negative magnetization [see Fig. 2(a)]. It occurs because the fM domain size increases infinitely as M approaches zero, and the coercive field also increases effectively [4] making the measuring field of 100 Oe too small and too ineffective to reverse the magnetization along the a axis. In contrast, far from the T_{comp} , when the coercive field is small enough, the FM moment exhibits a coherent rotation [see Fig. 2(c)] where at $T = 80$ K the easy magnetic axis is fixed along the a axis while at 100 K it is along the c axis]. The measured magnetization component $M(\theta)$ along \mathbf{H} follows nearly a simple angular dependence of $|\cos \theta|$ observed in ferromagnets with a strong uniaxial anisotropy [20]. At the intermediate temperature of 60 K, when the coercive field is comparable in value with an applied field, the negative magnetization and abrupt switching over to the positive one occur. In addition, a huge hysteresis in magnetization around the hard c axis occurs during \mathbf{H} rotation in the ac plane [see Fig. 2(b)].

In order to examine the magnetization hysteresis loops for different metastable spin configurations that occur in proximity of the first-order transition at T_{comp} , two different FC protocols were exploited: (1) FC in 10 kOe from 300 to 10 K and then warming to the given temperature T , and (2) FC in 10 kOe from 300 K to a given T , below called

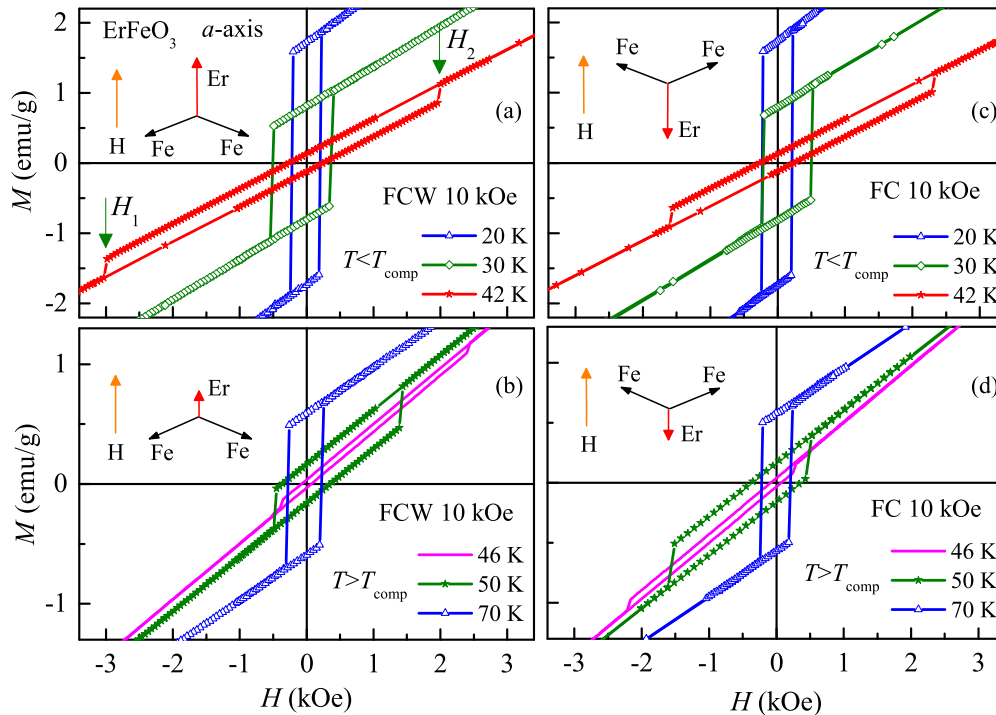


FIG. 3. Magnetization hysteresis loops of ErFeO_3 , in an extended scale, measured in the field up to 10 kOe applied along the a axis at $T < T_{\text{comp}} = 45$ K [(a), (c)] and at $T > T_{\text{comp}}$ [(b), (d)] after different cooling procedures: FC in 10 kOe from 300 to 10 K and then warming to the given T (abbreviated in the figure as FCW), and FC in 10 kOe from 300 K to given T (abbreviated in the figure as FC). The possible spin configurations for the case of low applied fields depending on cooling protocol are shown.

FCW and FC, respectively. Following FC protocol, one can fix at $T > T_{\text{comp}}$ the equilibrium spin configuration (with the net FM moment aligned along applied field H), while at $T < T_{\text{comp}}$, the metastable state characterized by the opposite FM moment at small field H is realized. On the contrary, the FCW procedure restores the equilibrium state at $T < T_{\text{comp}}$ and induces the metastable one at $T > T_{\text{comp}}$ [see the possible spin configurations for the case of low applied fields illustrated in Fig. 3]. The metastable states induced by FC/FCW may exist in the limited temperature region below/above T_{comp} , restricted by jumps in $M(T)$ curves, presented in Fig. 1(a). The $M(H)$ loops recorded with both protocols in magnetic fields up to 10 kOe applied along the a axis are shown in Fig. 3 in an extended scale for selected temperatures below [Figs. 3(a) and 3(c)] and above T_{comp} [Figs. 3(b) and 3(d)]. They comprise a linear field-dependent AFM contribution and the rectangular FM loops exhibiting the abrupt FM moment reversals going through the 180° domain wall motion [4] at the switching fields H_1 and H_2 that exhibit the true coercive fields [21]. As T_{comp} is approached with increasing T [see Fig. 3(a)], the $M(H)$ loop widens and its center shifts to the negative field, representing an increase in average coercive field $H_C = (H_2 - H_1)/2$ and emergence of the negative EB field defined as $H_{\text{EB}} = (H_1 + H_2)/2$. Immediately, after crossing T_{comp} , the loop shift suddenly reverses to the positive fields, signifying the positive EB, and then with increasing T the loop becomes narrow and symmetric, i.e., the EB disappears [see Fig. 3(b)]. A very similar evolution in hysteresis loop performed with FC is observed with decreasing T , namely, the loop shift changes from the negative field at $T > T_{\text{comp}}$ [Fig. 3(d)] to the positive one at $T < T_{\text{comp}}$ [Fig. 3(c)]. Let us compare two

loops recorded at $T = 50$ K with different cooling protocols. It appears that the FCW loop [recorded after crossing T_{comp} ; see Fig. 3(b)] shows a positive EB, while the FC loop [without T_{comp} overpass; see Fig. 3(d)] shows the negative EB with nearly the same $|H_{\text{EB}}|$ and H_C values. This verifies that the change of EB sign from negative to positive is induced by the crossing T_{comp} . It is also evidenced that the positive EB results from the metastable state (emerged during FCW across the T_{comp}) with FM moment opposite to that in the equilibrium state, stabilized during FC. Additionally, we measured the loop at $T = 50$ K following FC with $H = -10$ kOe (not presented) which shows the opposing symmetric shift as compared with that obtained for FC with $H = +10$ kOe, being almost identical to the loop recorded following FCW with $H = +10$ kOe. This proves the opposed FM moment orientation in the case of FCW. Consequently, there is an analogy with conventional EB, where the direction of the loop shift is changeable by the polarity of the external magnetic field. In ErFeO_3 , for such role pretends the reversal of the net FM moment at crossing T_{comp} . This is well demonstrated in Figs. 4(a) and 4(b) by the temperature variation of the coercive fields H_1 and H_2 measured in both FCW and FC regimes. Both H_1 and H_2 show a discontinuity across T_{comp} , and interestingly they mutually replace each other in different protocols, so for instance the $H_1(T)$ obtained with FCW is the mirror image of $H_2(T)$ obtained following FC. Such a behavior suggests that the unidirectional EB anisotropy, whatever its microscopic origin, is determined by the preceding thermal history.

Figures 4(c) and 4(d) summarize H_C and H_{EB} data recorded following both FCW and FC protocols in the temperature

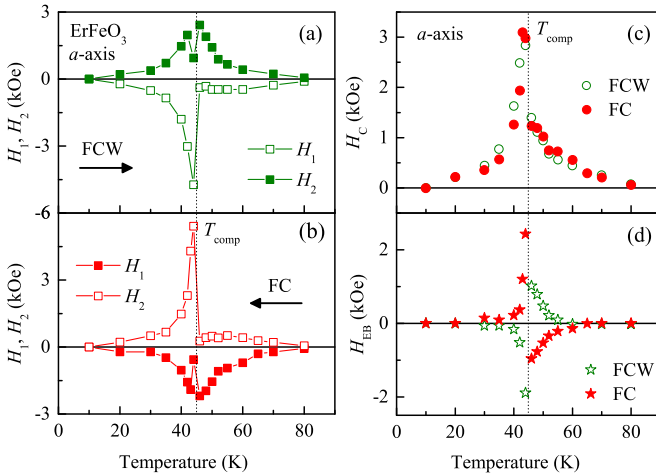


FIG. 4. (a), (b) Temperature variation of coercive fields H_1 and H_2 at the first and second magnetization reversals, respectively, obtained following different cooling procedures: FC in 10 kOe from 300 to 10 K and then warming to the given T (abbreviated in the figure as FCW), and FC in 10 kOe from 300 K to given T (abbreviated in the figure as FC). (c), (d) Average coercive field H_C (c) and exchange-bias field H_{EB} (d) around the compensation point T_{comp} , obtained for the FCW and FC protocols. Remarkably, both the coercive H_1 and H_2 fields, and the EB field obtained with FCW exhibit the mirror behavior of those obtained with FC.

interval 10–80 K. It appears that the average coercive field H_C does not depend on the cooling protocol and shows different behavior at T above and below T_{comp} . It diverges at temperatures slightly below T_{comp} , where the Er paramagnetic moment dominates and remains limited at $T > T_{comp}$ when the Fe canted FM moment prevails. Since an increase in H_C at T_{comp} is believed to be governed mainly by the increase of the FM domain size due to the vanishing of the net FM moment [4], one can suppose that the domain structure above and below T_{comp} is different. Such feature may explain the observed jump of ~ 1.5 kOe in H_C at T_{comp} , which is a hallmark of the first-order transition. The $H_{EB}(T)$ dependences, shown in Fig. 4(d), reveal several features: (i) The originally negative EB increases on approaching T_{comp} for both FCW and FC protocols and changes sign to a positive value across T_{comp} . (ii) At each temperature in the proximity of T_{comp} , the sign of EB can be switched by choosing either first or second protocol, so that the $H_{EB}(T)$ dependence recorded with FCW is the mirror image of that obtained with FC. (iii) The H_{EB} , revealing different signs in different cooling processes, diverges at $T < T_{comp}$, while its magnitude is restricted above T_{comp} . The fast increase of H_{EB} in the vicinity of T_{comp} may be clarified in terms of conventional EB where H_{EB} is inversely proportional to the net moment of the soft FM component [17]. Hence, the rapid change in H_{EB} at $T < T_{comp}$ is associated with the significant variation in M below T_{comp} [see Fig. 1(c)]. Moreover, the H_{EB} quickly disappears with lowering T as the net FM moment becomes too large to be pinned out by the AFM component. Apparently, the EB sign is determined by the direction of the soft FM moment, as reported for compensated ferrimagnets [7, 11], while in conventional EB it is linked to the sign of the interfacial interaction [22]. One can see that the EB

sign is generally negative in the equilibrium state, predominant at T above T_{comp} in the case of FC and below T_{comp} for the FCW. It always becomes positive immediately after crossing T_{comp} , when the metastable opposite FM moment appears at the first-order transition, illustrated in the inset to Fig. 1(a). Hence, we propose that the unique EB behavior, shown in the $H_{EB}-T$ plane, exhibiting two coexisting states with H_{EB} of different sign, is due to the first-order nature of the transition at T_{comp} . In analogy with traditional EB involving a FM/AFM interface, one can consider two interacting sublattices in ErFeO_3 , where the Er sublattice possesses the pinned FM component and the Fe one plays the role of the strongly anisotropic AFM layer. A similar model was employed recently for explaining the field-cooled dependent sign of EB in $\text{La}_{1-x}\text{Pr}_x\text{CrO}_3$ [11]. However, in distinct contrast to the conventional EB, no cooling field dependence of EB and no training effect were observed in ErFeO_3 single crystal.

Noteworthy, Webb *et al.* [7] have pointed out in 1988 the possible origin of EB anisotropy in compensated fMs. According to Ref. [7], the unidirectional anisotropy $H_{EB} \sim (M_A - M_B)^{-1}$ occurs at T_{comp} of fMs comprising two AFM coupled sublattices, A and B , with opposite moments. The H_{EB} is in fact a magnetic field at which the net FM moment reverses to minimize the energy state, while in the case of existence of coercivity it is the position of the center of the hysteresis loop. This model may describe basically the EB behavior observed in ErFeO_3 , which is a microscopically homogeneous fM exhibiting opposing Fe^{3+} and Er^{3+} spins within the unit cell and reveals a divergence in coercive field H_C at the T_{comp} (in contrast, the inhomogeneous fM system shows a collapse in H_C at T_{comp} , according to the classification of Webb *et al.* [21]). Namely, the H_{EB} becomes noticeable at small enough net magnetic moment ($M_A - M_B$) and it diverges at T_{comp} , according to the above proportionality. Moreover, the sign of H_{EB} is determined by the direction of the moment ($M_A - M_B$) with respect to the applied field H . It appears that H_{EB} normally is negative in the case of equilibrium spin configuration (FM moment is aligned along external field H), while it becomes positive in the metastable state with FM moment pointing to the direction opposite to the applied field.

To summarize, we have shown that ErFeO_3 orthoferrite exhibits a variety of the EB behavior. The EB appears in the vicinity of the compensation point, increases on approaching T_{comp} , and changes sign across T_{comp} . Both H_{EB} and H_C fields diverge below T_{comp} and they are restricted above T_{comp} . The EB was found to depend crucially on thermal history: (i) Its sign is generally negative for T above T_{comp} in the case of FC and below T_{comp} for the FCW. (ii) For both FC and FCW it becomes positive immediately after crossing T_{comp} . Hence, changing the cooling/warming protocol switches the EB sign for the same $|H_{EB}|$ and H_C values. The negative EB is compatible with the equilibrium spin configuration and the positive one with the metastable state. This relevant feature apparently reminds one of the possibility of electric-field-induced switching of the EB sign in a magnetoelectric $\text{Cr}_2\text{O}_3/\text{CoPt}$ heterostructure [23].

This work was partly supported by the Polish NCN Grant No. 2014/15/B/ST3/03898.

- [1] J. A. de Jong, A. V. Kimel, R. V. Pisarev, A. Kirilyuk, and Th. Rasing, *Phys. Rev. B* **84**, 104421 (2011).
- [2] H. Shen, Z. Cheng, F. Hong, J. Xu, S. Yuan, S. Cao, and X. Wang, *Appl. Phys. Lett.* **103**, 192404 (2013).
- [3] Ya. B. Bazaliy, L. T. Tsymbal, G. N. Kakazei, A. I. Izotov, and P. E. Wigen, *Phys. Rev. B* **69**, 104429 (2004).
- [4] L. T. Tsymbal, G. N. Kakazei, and Ya. B. Bazaliy, *Phys. Rev. B* **79**, 092414 (2009).
- [5] W. G. Koehler, E. O. Wollan, and W. K. Wilkinson, *Phys. Rev.* **118**, 58 (1960).
- [6] G. Deng, P. Guo, W. Ren, S. Cao, H. E. Maynard-Casely, M. Avdeev, and G. J. McIntyre, *J. Appl. Phys.* **117**, 164105 (2015).
- [7] D. J. Webb, A. F. Marshall, A. M. Toxen, T. H. Geballe, and R. M. White, *IEEE Trans. Magn.* **24**, 2013 (1988).
- [8] P. D. Kulkarni, A. Thamizhavel, V. C. Rakhecha, A. K. Nigam, P. L. Paulose, S. Ramakrishnan, and A. K. Grover, *Europhys. Lett.* **86**, 47003 (2009).
- [9] S. Venkatesh, U. Vaidya, V. C. Rakhecha, S. Ramakrishnan, and A. K. Grover, *J. Phys.: Condens. Matter* **22**, 496002 (2010).
- [10] R. P. Singh, C. V. Tomy, and A. K. Grover, *Appl. Phys. Lett.* **97**, 182505 (2010).
- [11] K. Yoshii, *Appl. Phys. Lett.* **99**, 142501 (2011).
- [12] R. Padam, S. Pandya, S. Ravi, A. K. Nigam, S. Ramakrishnan, A. K. Grover, and D. Pal, *Appl. Phys. Lett.* **102**, 112412 (2013).
- [13] A. K. Nayak, M. Nicklas, S. Chadov, P. Khuntia, C. Shekhar, A. Kalache, M. Baenitz, Yu. Skourski, V. K. Guduru, A. Puri, U. Zeitler, J. M. D. Coey, and C. Felser, *Nat. Mater.* **14**, 679 (2015).
- [14] P. Nordblad, *Nat. Mater.* **14**, 655 (2015).
- [15] K. Chen, D. Lott, F. Radu, F. Choueikani, E. Otero, and P. Ohresser, *Sci. Rep.* **5**, 18377 (2015).
- [16] W. H. Meiklejohn and C. P. Bean, *Phys. Rev.* **102**, 1413 (1956).
- [17] J. Nogués, J. Sort, V. Langlais, V. Skumryev, S. Suriñach, J. S. Muñoz, and M. D. Baró, *Phys. Rep.* **422**, 65 (2005).
- [18] G. Gorodetsky, B. Lüthi, T. J. Moran, and M. E. Mullen, *J. Appl. Phys.* **43**, 1234 (1972).
- [19] J.-S. Jung, A. Iyama, H. Nakamura, M. Mizumaki, N. Kawamura, Y. Wakabayashi, and T. Kimura, *Phys. Rev. B* **82**, 212403 (2010).
- [20] F. Y. Yang, C. L. Chien, E. F. Ferrari, X. W. Li, Gang Xiao, and A. Gupta, *Appl. Phys. Lett.* **77**, 286 (2000).
- [21] D. J. Webb, A. F. Marshall, Z. Sun, T. H. Geballe, and R. M. White, *IEEE Trans. Magn.* **24**, 588 (1988).
- [22] J. Nogués, D. Lederman, T. J. Moran, and I. K. Schuller, *Phys. Rev. Lett.* **76**, 4624 (1996).
- [23] P. Borisov, A. Hochstrat, X. Chen, W. Kleemann, and C. Binck, *Phys. Rev. Lett.* **94**, 117203 (2005).